SAND2000-1904J

Mass Transport in the Epitaxial Lateral Overgrowth Of Gallium Nitride

(to be submitted to Journal of Crystal Growth, June 2000)

Christine C. Willan, Michael E. Coltrin, and Jung Han
Sandia National Laboratories
Albuquerque, NM 87185

ABSTRACT

We have investigated lateral transport mechanisms in Epitaxial Lateral Overgrowth (ELO) of GaN grown by Metal Organic Chemical Vapor Deposition. Portions of a pre-grown GaN buffer layer are patterned with a dielectric mask material, silicon nitride. Further growth of GaN occurs selectively on exposed areas of the underlying buffer layer, and not on the dielectric material. Growth-rate enhancement on the exposed GaN is observed due to lateral transport of material from the masked regions. We describe experiments to distinguish whether the lateral transport of material occurs via gas-phase diffusion or surface diffusion on the mask itself or on the epitaxial material . Deep trenches were etched into the wafer prior to the ELO growth, designed to interrupt lateral transport if it were occurring by diffusion along the surface. ELO growth rate profiles on exposed line patterns and on larger area blanket growth zones were examined with and without the trenches. Growth profiles were virtually identical independent of the presence of the trench features. These results indicate that gas-phase diffusion dominates the transport of material during GaN ELO.

1. Introduction

Selective area growth (SAG) of compound semiconductor thin films by metal organic chemical vapor deposition (MOCVD) has found a range of applications. In some III-V systems, it is found that material will not grow on regions of a wafer covered by a dielectric such as silicon dioxide or silicon nitride. Thus, if a wafer is patterned to cover some regions (masked zones) of an underlying epitaxial substrate, growth will proceed selectively only on the exposed (unmasked) regions. SAG can be used for lateral dimension control and to achieve thickness and composition variation across the wafer, thus tailoring device characteristics. A useful overview of SAG is found in Ref. [1].

Gallium nitride (GaN) has emerged as a useful semiconductor because of its unique combination of optoelectronic, microelectronic, piezoelectric, mechanical, and chemical properties. These properties make GaN suitable for, among other things, LEDs and lasers that emit in the blue and UV regime, high temperature/power/frequency electronics for use in adverse environments, and mixed opto-mechanical-electronic devices for multifunctional integrated microsystems.

Because there is currently no lattice-matched substrate available for single-crystal epitaxial growth, MOCVD GaN thin films grown on sapphire and SiC contain a very high density of defects and dislocations. A variation of selective area growth finds particular utility in growth of high quality GaN thin films [2-27]. In this variation, a GaN buffer layer is grown on sapphire, SiC, or Si followed by deposition of a blanket layer of dielectric material. The dielectric is photolithographically patterned and then etched exposing portions of the underlying GaN buffer layer, usually arrayed in long parallel lines separated by wider zones of the unetched

DISCLAIMER

DISCLAIMER

Portions of this document may be illegible in electronic image products. Images are produced from the best available original document.

mask. The wafer is returned to the MOCVD growth chamber for continued GaN growth, which proceeds selectively only from the exposed GaN regions. Growth of GaN continues vertically and laterally over the mask material. It is found that the defect density of the laterally overgrown material can be two orders of magnitude smaller than for the normal, unpatterned GaN growth directly on a GaN buffer. This technique for production of epitaxial quality GaN has been referred to by a number of different names by different researchers. We will denote this technique Epitaxial Lateral Overgrowth (ELO) when discussing growth on patterned lines (small openings, < 10 μm in width), and will refer to the "blanket" selective growth on larger areas (hundreds of microns) as Selective Area Growth (SAG).

In SAG and ELO a growth-rate enhancement is observed on the exposed regions, especially those areas adjacent to the mask, relative to the rate of unpatterned growth. Because growth proceeds selectively only on the exposed epilayer the precursors, particularly the group-III species which are rate-limiting, are not consumed over the masked regions. The "excess" reagents undergo lateral transport from the masked to the exposed regions, contributing to the observed growth-rate enhancement. However, the mechanism of lateral mass transport of material has been the subject of some contention over the years. There are two separate aspects of lateral mass transport to be addressed: transport of material from the masked region and transport of material across the epitaxial material. In both cases, the issue is whether the transport takes place on the surface or in the gas phase.

The earliest studies of SAG tended to conclude that growth-rate enhancement was due to lateral surface diffusion of reactants on the dielectric mask itself [28-31]. The surface diffusion length on the mask was assumed to be very large, perhaps hundreds of microns or more. Any molecule landing on the mask within this length was assumed to diffuse to the exposed epilayer

and react, thus explaining the selectivity and the growth rate enhancement. However, more recently many authors have explicitly concluded that diffusion lengths on the mask are very short [1, 32-38]. Under these conditions the dominant lateral mass transport mechanism from the masked region, for distances greater than a few (< 2 or 3) microns, is usually attributed to gas-phase diffusion [1, 32, 33, 36-46].

It is generally concluded that *short-range* diffusion (in the range of 1 to 10 μm) on the surface of the epitaxial material occurs during III-V growth [1, 15, Kitamura, 1995 #49, 17, 20, 34, 45, 47-49]. This short-range diffusion is important, and almost assuredly responsible for the observed growth of smooth facets on the epitaxial material. However, for much longer distances (> 10 μm), it is likely that the dominant mass transport mechanism for epitaxial growth is gas-phase diffusion [39, 48-50]. This was made very clear in experiments by Gibbon [50] and Sasaki [49], in which deep trenches were placed in the epitaxial material. Growth rate enhancement profiles were examined with and without the presence of the trenches and were found to be virtually identical. If mass transport on the epitaxial surface had been the dominant mechanism, the trenches would have perturbed the measured growth profiles. (We are not aware of experiments where trenches were placed in the mask for a similar direct test of surface diffusion on the mask material.)

Gallium nitride grown by ELO exhibits smooth facets, typically exposing the (0001) basal plane bounded by $(1\bar{1}01)$ or $(11\bar{2}n)$ $(n \approx 2)$ faces, depending upon the orientation of the exposed stripes relative to the underlying sapphire substrate. The observation of smooth facets certainly implies the importance of surface diffusion at the small length scales of the ELO features [10, 17, 20]. However, one report argues against surface diffusion on the epilayer between facets, attributing the growth habit to local thermodynamic effects [13].

For GaN ELO, transport of material from the dielectric mask to the exposed regions has not been tested directly. Indeed, roughly equal numbers of GaN ELO articles have assumed gas-phase transport from the mask [12, 18, 21, 51] or have assumed surface diffusion from the mask [8, 11, 15].

This paper describes a set of experiments to test the relative importance of surface versus gas-phase lateral mass transport of material for GaN SAG and ELO. The experiment is similar in design to that of Gibbon [50] and Sasaki [49] in that deep trenches are employed to interrupt transport of material on the surface, if that mechanism is operative. In this case, we place such trenches within the exposed epitaxial region, but also in the masked region to test surface versus gas-phase transport on both regions of the wafer. Si(111) wafers were used as substrates in this work rather than sapphire, because methods are readily available for etching high aspect ratio trenches into Si, and that capability is not available for sapphire. A number of examples of GaN growth on Si(111) substrates have been reported [22-27].

2. Experiment

Silicon (111) wafers were patterned using standard photolithography techniques, and portions of the wafer were etched [52] to form trenches 10 μm wide and 80 μm deep. After etching, a GaN base layer was grown in a low pressure MOCVD rotating disk reactor. The base layer starts with a 30 nm high-temperature (HT) AlN buffer layer grown at 1100 °C and a reactor pressure of 30 torr. This was followed by a 50 nm layer of AlGaN and a 50 nm layer of GaN grown at 1080 °C and a reactor pressure of 40 torr. Trimethyl alumnium (TMA), trimethyl gallium (TMGa), and ammonia (NH_3) were used as the precursors for the growth. The flow rates were 1.46 sccm, 3.89 sccm, and 1800 sccm for the AlN growth respectively. The flow rates were 1.94 sccm, 3.89 sccm, and 2500 sccm for the AlGaN growth respectively. The TMGa flow

rate was 3.89 sccm and the NH_3 flow rate was 2500 sccm for the GaN growth. After the base layer growth, 1000 Å of plasma enhanced chemical vapor deposition (PECVD) Si_3N_4 was deposited on the etched substrate and was then patterned using conventional photolithography techniques. After patterning the exposed mask was etched away using a plasma assisted reactive ion etch (RIE) system to expose the underlying GaN base layer. The wafer was then put back in the MOCVD chamber for the SAG. This growth was completed without any additional buffer layers, and 0.5 μm of GaN was grown at a temperature of 1050 °C with a TMGa flow rate of 3.89 sccm and an NH_3 flow rate of 6000 sccm. The reactor pressure was 140 torr.

During the processing, a difficulty was encountered patterning the Si_3N_4 mask. Spinning uniform photoresist (PR) on a surface with 80 μm height variations is very difficult. In our experiment, the PR pulled away from the edges of the Si mesas; as a result ~0.5 μm of the dielectric mask was etched away along the edges of each trench, as well as in the desired areas during the reactive-ion etching step. This exposed GaN was thus an area for additional, parasitic GaN growth during the SAG step. This undesired trench-edge effect occurred to some degree for all of the patterns. It is illustrated in Figure 1, which shows a scanning electron micrograph (SEM) of the excess undesired growth at the edge of the mesas.

The growth profile data from the SAG experiments was obtained using an Alphastep 500 Profilometer. This method is an effective way to measure growth enhancement over the range of 500 μm with a vertical range of ~3 μm. The data for the ELO patterns was taken using a scanning electron microscope (SEM). For these experiments the base width of each feature and the width of the top basal plane (if present) were measured in top view. The cross-sectional area was then calculated assuming the angles of 58.41° for the $\{1\bar{1}22\}$ faces and 61.96° for the $\{1\bar{1}01\}$ faces, depending upon the orientation of the patterned ELO with respect to the substrate.

3. Results

3.1 Selective Area Growth (SAG) experiments

The first experiment to be described is the control pattern for standard GaN SAG, and will be referred to as the "No Trench" pattern. The unit cell for the SAG pattern, shown schematically in Figure 2a, has a square growth zone 500 μm x 500 μm, surrounded on all sides by 500 μm of Si_3N_4 mask. This unit cell and the two trenched patterns discussed later were arranged in 6 x 6 arrays for redundancy. The expected growth profile across the exposed epitaxial region for this type of pattern has been previously shown for GaN [11, 51, 53], with increased growth thickness at the edges of the epilayer, adjacent to the mask. Figure 3 shows the profile measured for half of the growth zone. This scan, labeled No Trench, begins from the masked area on the left and proceeds toward the growth zone on the right. The profile definitely shows the expected growth enhancement near the mask edge. Clearly, mass has been transported laterally from the mask region to the outer edge of the exposed epilayer, and continuing inward to the center region of the GaN.

One possible transport scenario would be that the growth precursor adsorbs on the mask, and lateral transport occurs via diffusion **on the mask** surface. The excess of reactants reaching the epilayer from the side would lead to a growth enhancement profile as seen in Figure 3. Presumably, surface diffusion **on the epilayer** continues the surface transport of material toward the center of the pattern. Thus, this surface transport scenario has two separate portions that could conceivably be tested, i.e., (1) lateral surface transport along the mask and (2) lateral surface transport along the surface of the GaN epilayer. Placement of a deep trench in either the masked region or in the GaN epilayer should interrupt surface transport steps (1) and (2), respectively, leading to a dramatic change in the SAG growth profile.

If the dominant mechanism for lateral transport of material from the mask region and continuing across the exposed epilayer toward the center is by gas-phase diffusive transport, then placement of deep trenches into either surface should have a negligible affect on the SAG growth profile. The next two sets of experiments performs these tests.

The SAG "Mask Trench" pattern is shown schematically in Figure 2b, which is designed to test lateral mass transport from the masked regions to the growth zone. The unit cell for the Mask Trench pattern uses a growth zone similar to the control pattern, but separates the exposed GaN region from the adjacent masked area by trenches 10 μm wide and 80 μm deep. Separating the growth zone from the mask with trenches effectively removes the possibility of any reactants from the mask area reaching the growth region if surface diffusion is the dominant method of lateral transport. If surface diffusion on the mask dominates the transport of reactants, the expected growth profile on the exposed region would be flat with no growth enhancement at the edges of the square. In addition, the only reactants available for growth with this method of transport would be those molecules that land directly on the exposed growth surface; this would also result in much less overall deposition across the total exposed growth area.

If lateral gas-phase diffusion from the masked region is dominant, the resulting growth from the pattern shown in Figure 2b should basically match the original profile from the No Trench pattern of Figure 2a. The measured profile for this experiment is shown in Figure 3, labeled "Mask Trench." The Mask Trench results are somewhat complicated by the presence of the unintended, parasitic growth of GaN at the edges of the trench (mentioned in the Experiment section).

Beginning from the left side of the Mask Trench scan seen in Figure 3, the trace starts over the masked zone, where there is no growth (as expected). The first feature encountered as

the scan moves to the right is the parasitic growth at the trench edge adjacent to the growth zone. This feature is labeled P in the schematic drawn below the scan in Figure 3. The mesa created by the trench should ideally have been completely covered in Si_3N_4, so no GaN growth would occur there. However, because of the patterning issues discussed earlier, the mask material did not reach the edge allowing the "extra GaN growth." For purposes of comparing between the three growth profiles in Figure 3, this parasitic feature should be disregarded. As the Mask Trench scan continues to the right, the dip corresponds to the trench, followed by the exposed epitaxial growth region.

The Mask Trench scan across the epitaxial layer, in spite the undesired growth, shows the same basic SAG growth rate enhancement profile as seen in the No Trench case. The presence of the trench between the masked area and the exposed epitaxial region does not significantly alter the amount of lateral mass transport. This result offers strong evidence that the long-range (tens to hundreds of microns) lateral transport mechanism is by gas-phase, rather than surface, diffusion.

The SAG "Epi Trench" pattern is shown schematically in Figure 2c. This pattern places a trench, 10 μm wide and 80 μm deep, a distance 50 μm in from the edge of the growth zone as well as separating all other sides from the mask by similar trenches. The Epi Trench will serve as a barrier for any reactants diffusing along the surface of the epilayer. If surface diffusion is the controlling lateral transport mechanism, the resulting cross sectional profile should have two parts. On the left side of the trench, adjacent to the large masked section, there will be a very thick growth feature on the small exposed region. This feature would be attributed to the reactants transported from the mask and on the growth surface. However, continued transport inward toward the center of the epi region would be cut off if the transport is occurring on the

surface of the epilayer. Thus, one would expect that to the right of the trench the growth would be flat and much less thick, because its only source of precursors would be those landing directly on the growth zone and on the small area of mask to the right of the growth zone. If gas phase diffusion is the controlling mechanism the profile of the growth should be basically the same as in the "No Trench" pattern; the trench 50 μm from the edge would not affect the growth enhancement.

Figure 3 displays the profile of the SAG grown on the "Epi Trench" pattern. From left to right, the scan shows the masked zone followed by 50 μm-wide zone of exposed GaN growth, followed by the trench and then proceeds toward the remaining center section of growth. The profilometer scan from the Epi Trench pattern shows the same profile shape as the No Trench scan, with the obvious exception of the trench 50 μm from the mask edge. The presence of the trench does not affect the SAG growth enhancement profile, providing strong evidence that lateral gas-phase diffusion (rather than diffusion on the epilayer) is controlling the supply of reactants across the epilayer for distances over a few microns.

As discussed several times, an undesired difference between the "No Trench" pattern and the "Mask Trench" and "Epi Trench" patterns is that the latter two have 21 additional edges of undesired growth in the experimental unit cell, i.e., along the trench edges. This problem does not significantly affect the overall conclusions to be drawn from the data. However, quantitative comparison of the total amount of deposited material on the exposed epilayer between the three experiments requires that one take this into account.

The areas under the three curves shown in Figure 3 are 759 μm^2, 600 μm^2, and 628 μm^2 for the No Trench, Mask Trench, and Epi Trench patterns, respectively. Thus, the latter two trench patterns are nearly identical in the total amount of material deposited on the epilayer,

while roughly 20% more material was deposited in the No Trench scan over the exposed region. The No Trench experiment shows the larger amount of material deposited, presummably because it lacks the extra "sink terms" for the parasitic growth at trench edges.

It would be very difficult to quantitatively measure the amount of material deposited on each of the trench edges. So, in order to overlay the growth profiles for comparison, we simply scale the No Trench scan by a factor of 0.8 in Figure 4. The comparison clearly shows the three growth enhancement profiles are qualitatively the same, and it can be concluded that gas-phase transport is the controlling lateral mass transport.

3.2 Epitaxial Lateral Overgrowth (ELO) experiments

Another variation of the experiment described above is to pattern a series of Epitaxial Lateral Overgrowth (ELO) lines on the center region of the unit cell, rather than leaving the entire surface open, as in SAG. The pattern used for these experiments is shown schematically in Figure 5 a & b. The line pattern consists of alternating 4 μm-wide lines separated by 16 μm-wide mask stripes. Twenty-four exposed lines are patterned across the center region of each unit cell. Because ELO lateral growth rates are found to vary with the exposed stripe orientation (with respect to the underlying substrate) [9, 17, 18, 54], different regions of the wafer were designed with line patterns oriented perpendicular to one another. The two relevant orientations for lines in this system are the $[1\bar{2}0]$ GaN $\|$ $[1\bar{1}0]$ Si direction [55, 56] (which we shall denote as the 0° stripe orientation) and $[1\bar{1}00]$GaN $\|$ $[110]$ Si direction (called the 90° stripe orientation).

The grown ELO features exhibited flat facets, suggesting facile **short range** diffusion on the GaN crystal faces (diffusion lengths on the order of the size of the facets). Features growing

laterally from the 0° stripes consisted of "tents" of GaN $\{1\bar{1}01\}$ facets; the faster-growing (0001) basal plane was not present. Faster lateral overgrowth is seen from the 90° stripes, which exhibit $\{11\bar{2}2\}$ facets; these lines grow so fast laterally that they do not terminate in a point, but are bounded at the top by the (0001) basal plane.

Because large masked regions surround the ELO growth zones, significant "edge effects" are expected and seen. Plotted in Figure 6 is the cross-sectional area of the ELO line as a function of feature number, counting from 1 at the edge of the large mask sequentially inward. Results for the control experiment, without the trench diffusion barriers, are given by the + and × symbols for the 0° and 90° lines, respectively. In each case, the cross-sectional area is at a maximum for feature number 1 and drops monotonically to the center symmetry line. It is seen that the ELO growth rate is greater for the 90° orientation of the lines, consistent with the faster growth of the $\{11\bar{2}2\}$ facets observed many times [9, 17, 18, 54].

Similar in spirit to the experiments in the previous section, the ELO experiment was repeated with deep trenches etched into the mask adjacent to the first exposed GaN line pattern, which is shown schematically in Figure 5b. If surface diffusion dominates the lateral mass transport from the masked region, the ELO feature size distribution should be dramatically altered by the presence of the trenches. For a mask-surface transport mechanism, one would expect the features to be uniform in size across the entire patterned growth zone. In addition, the total amount of material deposited in the features should be less, because no "extra" precursors outside the trenched-in area would contribute to growth. For a gas-phase lateral transport mechanism, one would see a significant mask-edge effect. The same parasitic growth of GaN at the edge of the Mask Trenches was present in these experiments. Consequently the total amount of material available for growth on the ELO lines is slightly smaller in the trench experiments.

The cross sectional areas in the ELO No Trench experiment have been scaled by a factor of 0.85 to account for the difference in total deposition, which was chosen so that the inner-most features match in cross-sectional area.

Figure 6 shows the measured cross-sectional area of the features for this ELO Mask Trench experiment, the triangular and square symbols represent the 0° and 90° stripe orientations, respectively. The ELO feature-size distribution is virtually identical with and without the presence of the trenches. The significant edge enhancement is seen for both stripe orientations and the cross-sectional areas of the features are very similar. In addition, the faster growth of the 90° stripes compared to the 0° orientation is also observed in the trench experiment. This data is consistent with a gas-phase diffusion mode of lateral mass transport, and would rule-out long range (tens to hundreds of microns) diffusion on the surface of the mask itself.

In the previous section, we also tested long-range (> 10 μm) diffusive transport mechanisms on the epi layer in SAG. For the present ELO experiment, the exposed line features are too narrow to place a trench within the exposed GaN growth window. In addition, for the small dimensions of the epitaxial features (< 10 μm as compared to 500 μm in the SAG tests), one actually expects that surface diffusion on the facets is occurring in order to yield the flat crystal faces that are observed [1, 15, Kitamura, 1995 #49, 17, 20, 34, 45, 47-49]. Thus, there are no comparable Epi Trench experiments to be report in this ELO section.

4. Conclusions

Mechanisms for long-range (> 10 μm) lateral mass transport of material for GaN selective area growth (SAG) and epitaxial lateral overgrowth (ELO) were tested. For the SAG experiments, deep trenches were etched into the surface of the mask and into the exposed

epitaxial region as barriers to lateral transport if it were taking place on the surface of the mask or on the epitaxial material itself. SAG growth thickness profiles exhibited the same behavior with and without the presence of the trench features. A similar experiment placed a deep trench in the dielectric mask adjacent to exposed lines for ELO growth. The GaN ELO feature growth was also virtually unaffected by the presence of the trenches.

Both of these results argue strongly that growth rate enhancement seen in GaN SAG and ELO is a due to gas-phase diffusive transport of material. This has been the general conclusion for SAG in other compound semiconductor materials. This experimental result serves to confirm the assumptions in previous models of GaN SAG and ELO [5, 11, 53].

5. Acknowledgements

We gratefully acknowledge R. G. Shul and C. G. Willison of Sandia's Compound Semiconductor Research Laboratory for etching the Si wafers, J. J. Figiel and K. Waldrip for technical assistance in the MOCVD growth, and G. Lopez for valuable advice in patterning our wafers. This work was performed at Sandia National Laboratories and supported by the U. S. Department of Energy under contract number DE-AC04-94AL85000, with funding from the Office of Basic Energy Sciences, Division of Materials Science.

List of Figures

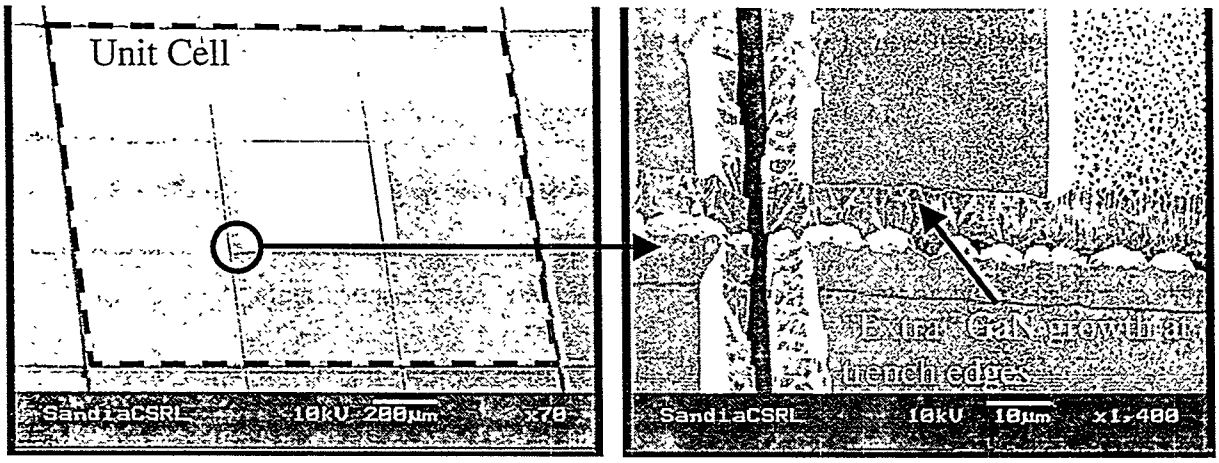
Unit Cell
SandiaCSRL 10kV 200µm x70
Extra GaN growth at trench edges
SandiaCSRL 10kV 10µm x1,400

(a) (b)

Figure 1

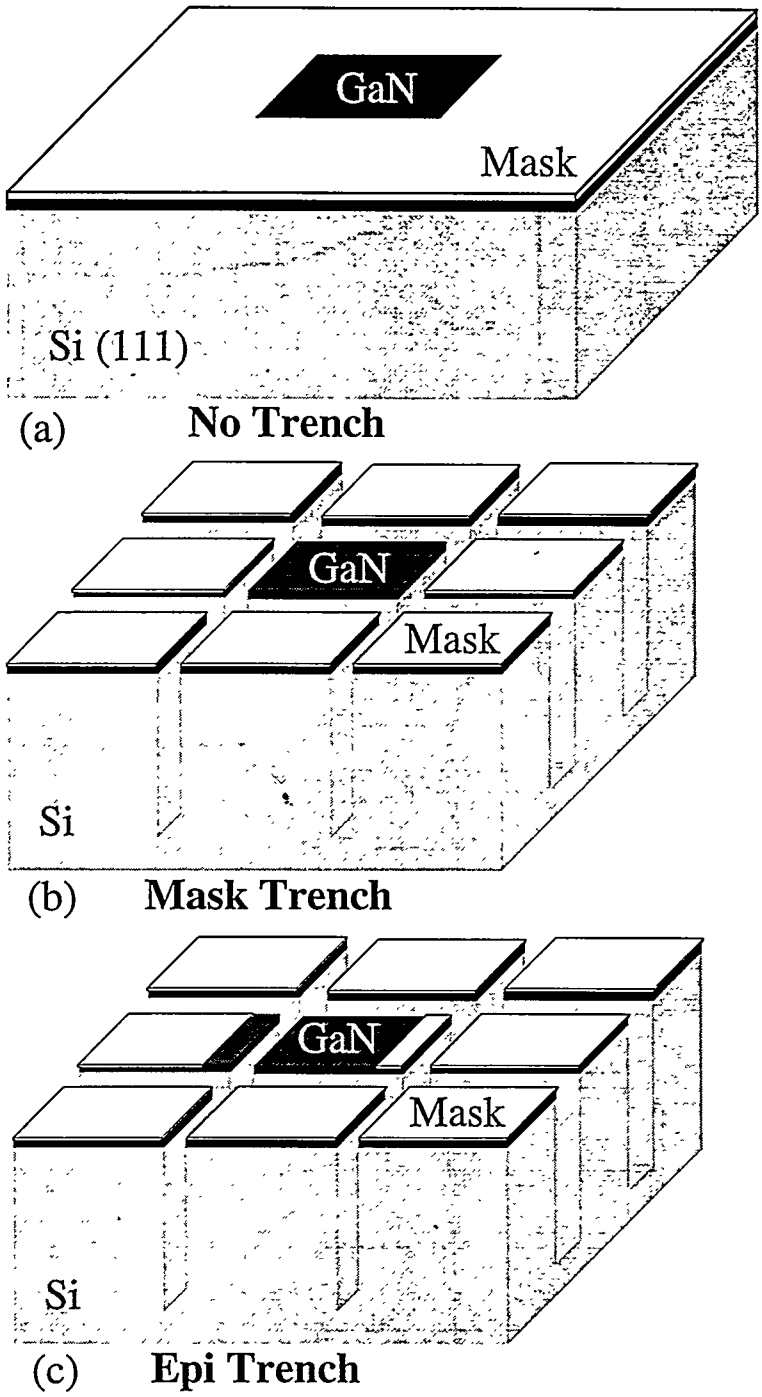
GaN
Mask
Si (111)
(a) No Trench
GaN
Mask
Si
(b) Mask Trench
GaN
Mask
Si
(c) Epi Trench

Figure 2

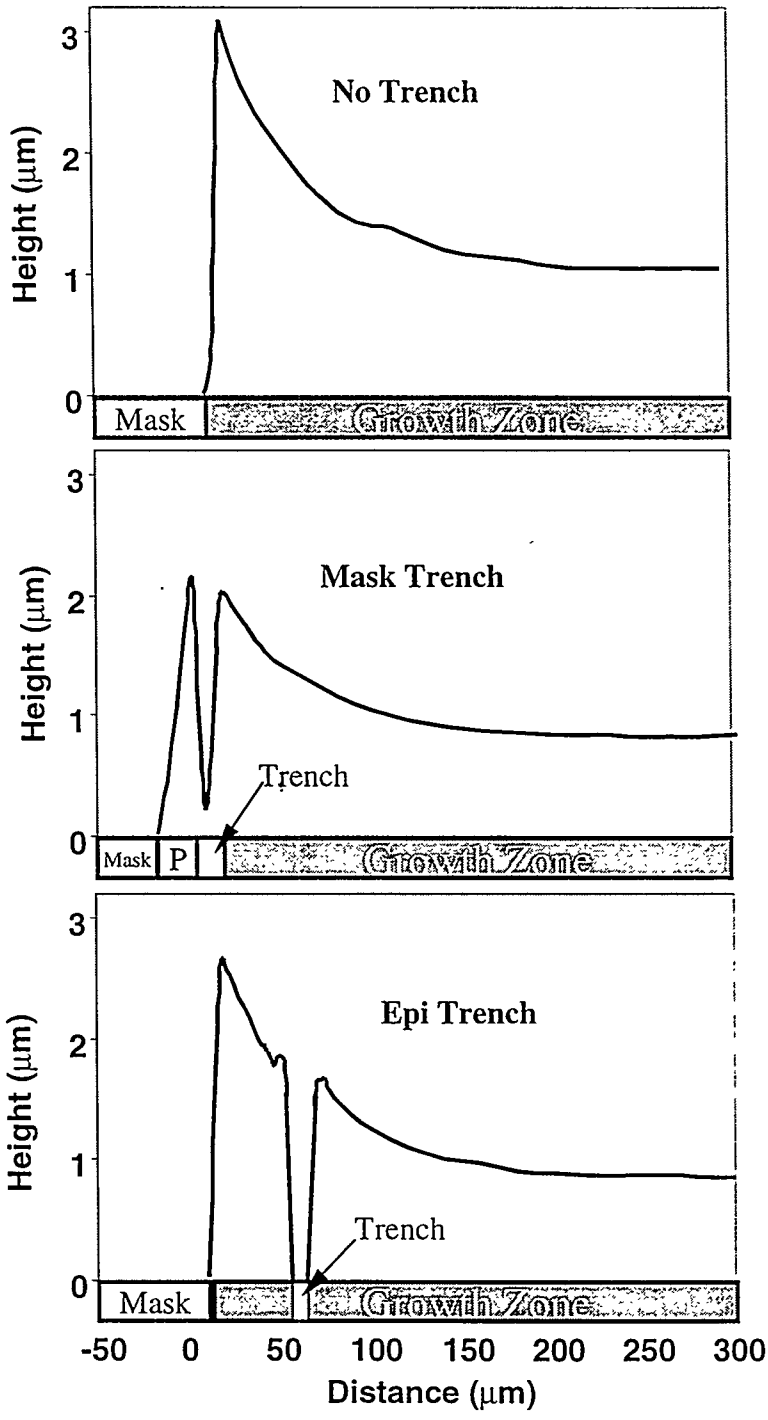
No Trench
Mask Trench
Epi Trench
Height (μm)
Distance (μm)
Mask
P
Trench
Growth Zone
0
1
2
3
-50
0
50
100
150
200
250
300

Figure 3

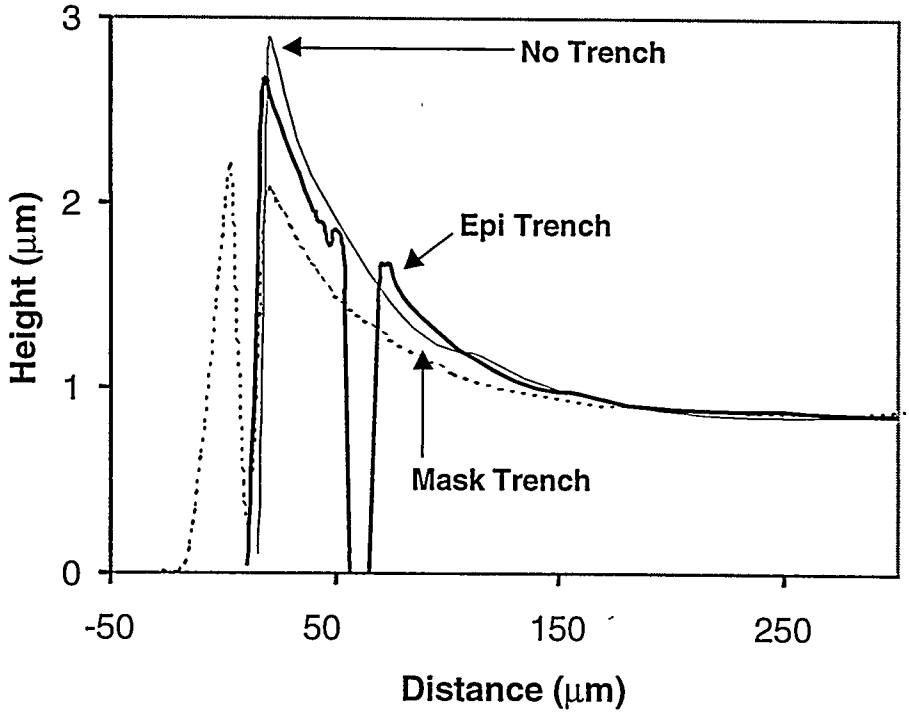

Figure 4

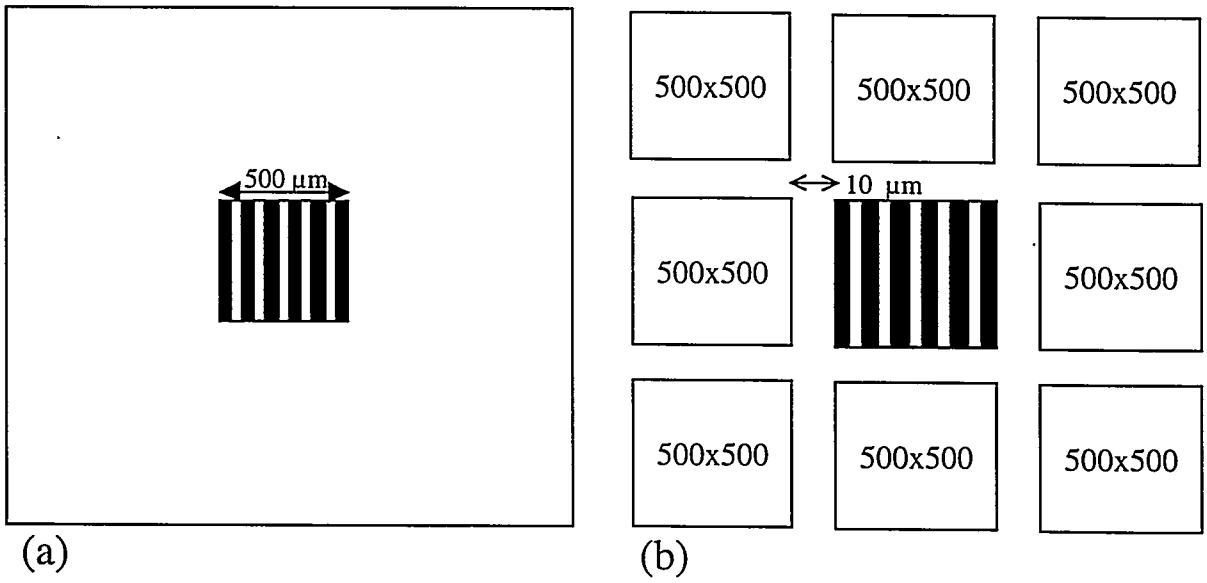

Figure 5

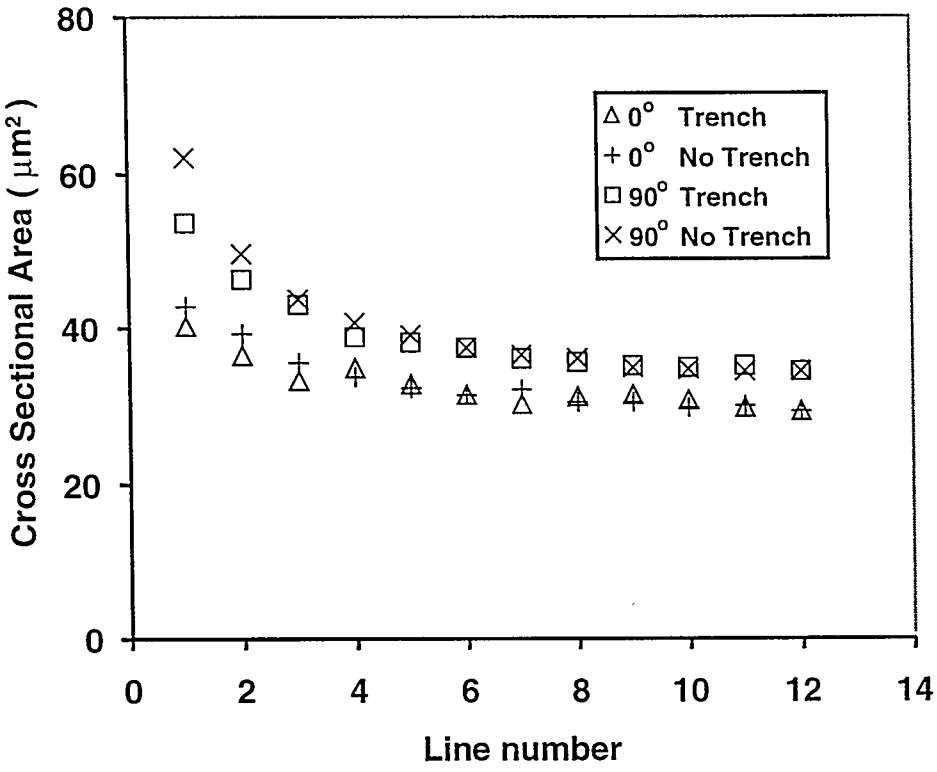
80
60
40
20
0
Cross Sectional Area (μm²)
0
2
4
6
8
10
12
14
Line number
Δ 0° Trench
+ 0° No Trench
□ 90° Trench
× 90° No Trench

Figure 6

References

1. R. Bhat, J. Cryst. Growth 120 (1992) 362.
2. T. Akasaka, Y. Kobayashi, S. Ando, N. Kobayashi, Appl. Phys. Lett. 71 (1997) 2196.
3. B. Beaumont, M. Vaille, G. Nataf, A. Bouille, J.C. Guillaume, P. Vennegues, S. Haffouz, P. Gibart, MRS Internet J. Nitride Semicond. Res. 3 (1998) 1.
4. S.F. Chichibu, H. Marchand, M.S. Minsky, S. Keller, P.T. Fini, J.P. Ibbetson, S.B. Fleischer, J.S. Speck, J.E. Bowers, E. Hu, U.K. Mishra, S.P. Denbaars, T. Deguchi, T. Sota, S. Nakamura., Appl. Phys. Lett. 74 (1999) 1460.
5. M.E. Coltrin, C.C. Willan, M.E. Bartram, J. Han, N. Missert, M.H. Crawford, A.G. Baca, MRS Internet J. Nitride Semicond. Res. 4 (1999) U602.
6. P. Fini, H. Marchand, J.P. Ibbetson, S.P. Denbaars, U.K. Mishra, J.S. Speck., J. Cryst. Growth 209 (1999) 581.
7. P. Fini, L. Zhao, B. Moran, M. Hansen, H. Marchand, J.P. Ibbetson, S.P. Denbaars, U.K. Mishra, J.S. Speck., Appl. Phys. Lett. 75 (1999) 1706.
8. S. Haffouz, B. Beaumont, P. Gibart, MRS Internet J. Nitride Semicond. Res. 3 (1998) 1.
9. D. Kapolnek, S. Keller, R. Vetury, R.D. Underwood, P. Kozodoy, S.P. DenBaars, U.K. Mishra, Appl. Phys. Lett. 71 (1997) 1204.
10. S. Kitamura, K. Hiramatsu, N. Sawaki, Jpn. J. Appl. Phys. 34 (1995) L1184.
11. X. Li, A.M. Jones, S.D. Roh, D.A. Turnbull, S.G. Bishop, J.J. Coleman, J. Electron. Mater. 26 (1997) 306.
12. H. Marchand, J.P. Ibbetson, P.T. Fini, X.H. Wu, S. Keller, S.P. Denbaars, J.S. Speck, U.K.Mishra, MRS Internet J. Nitride Semicond. Res. 4 (1999) U462.

13. H. Marchand, J.P. Ibbetson, P.T. Fini, X.H. Wu, S. Keller, S.P. Denbaars, J.S. Speck, U.K.Mishra, J. Cryst. Growth 195 (1998) 328.

14. H. Marchand, X.H. Wu, J.P. Ibbetson, P.T. Fini, P. Kozodoy, S. Keller, J.S. Speck, S.P. Denbaars, U.K.Mishra, Appl. Phys. Lett. 73 (1998) 747.

15. D. Marx, Z. Kawa, T. Nakayama, Y. Mihashi, T. Takami, M. Nunoshita, T. Ozeki., J. Cryst. Growth 189-190 (1998) 87.

16. H. Matsushima, M. Yamaguchi, K. Hiramatsu, N. Sawaki, J. Cryst. Growth 189 (1998) 78.

17. O.-H. Nam, T.S. Zheleva, M.D. Bremser, R.F. Davis, J. Electron. Mater. 27 (1996)

18. J. Park, A. Grudowski, C.J. Eiting, R.D. Dupuis, Appl. Phys. Lett. 73 (1998) 333.

19. S.J. Rosner, G. Girolami, H. Marchand, P.T. Fini, J.P. Ibbetson, L. Zhao, S. Keller, U.K. Mishra, S.P. DenBaars, J.S. Speck., Appl. Phys. Lett. 74 (1999) 2035.

20. T. Tanaka, K. Uchida, A. Watanabe, S. Minagawa, Appl. Phys. Lett. 68 (1996) 976.

21. T.S. Zheleva, O.-H. Nam, M.D. Bremser, R.F. Davis, Appl. Phys. Lett. 71 (1997) 2472.

22. S. Tanaka, Y. Kawaguchi, N. Sawaki, M. Hibino, K. Hiramatsu, Appl. Phys. Lett. 76 (2000) 2701.

23. Y. Kawaguchi, Y. Honda, H. Matsushima, M. Yamaguchi, K. Hiramatsu, N. Sawaki, Jpn. J. Appl. Phys. 37 (1998) L966.

24. Y. Kawaguchi, Y. Honda, M. Yamaguchi, N. Sawaki, K. Hiramatsu, Physica Status Solidi A 176 (1999) 553.

25. B.L. Ward, O.-H. Nam, J.D. Hartman, S.L. English, B.L. McCarson, R. Schlesser, Z. Sitar, R.F. Davis, R.J. Nemanich, Journal of Applied Physics 84 (1998) 5238.

26. Z. Mao, S. McKernan, C.B. Carter, W. Yang, a.S.A. McPherson, MRS Internet J. Nitride Semicond. Res. 4 (1999) U184.

27. W. Yang, S.A. McPherson, Z. Mao, S. McKernan, C.B. Carter, J. Cryst. Growth 204 (1999) 270.

28. C. Blaauw, A. Szaplonczay, K. Fox, B. Emmerstorfer, J. Cryst. Growth 77 (1986) 326.

29. Y. Takahashi, S. Sakai, M. Umeno, J. Cryst. Growth 68 (1984) 206.

30. Y.D. Galeuchet, P. Roentgen, V. Graf, Appl. Phys. Lett. 68 (1990) 560.

31. K. Hiruma, T. Haga, M. Miyazaki, J. Cryst. Growth 102 (1990) 717.

32. O. Kayser, J. Cryst. Growth 107 (1991) 989.

33. E. Colas, A. Shahar, B.D. Soole, W.J. Tomlinson, J.R. Hayes, C. Caneau, R. Bhat, J. Cryst. Growth 107 (1991) 226.

34. S.H. Jones, L.K. Seidel, K.M. Lau, M. Harold, J. Cryst. Growth 108 (1991) 73.

35. Y. Mishima, N. Kaida, M. Sugiyama, Y. Sugiyama, Y. Nakano, Electrochem. Soc. Proc. 98-23 (1998) 364.

36. K.-i. Yamaguchi, M. Ogasawara, K. Okamoto, Appl. Phys. Lett. 12 (1992) 5919.

37. K. Yamaguchi,K. Okamoto, Jpn. J. Appl. Phys. 32 (1993) 1523.

38. M.F. Zybura, S.H. Jones, J.M. Duva, J. Durgavich, J. Electron. Mater. 23 (1994) 1055.

39. T. Fujii, M. Ekawa, S. Yamazaki, J. Cryst. Growth 156 (1995) 59.

40. C. Caneau, R. Bhat, M.R. Frei, C.C. Chang, R.J. Deri, M.A. Koza, J. Cryst. Growth 124 (1992) 243.

41. C. Caneau, R. Bhat, C.C. Chang, K. Kash, M.A. Koza, J. Cryst. Growth 132 (1993) 364.

42. Y.D. Galeuchet,P. Roentgen, J. Cryst. Growth 107 (1991) 147.

43. A.M. Jones, M.L. Osowski, R.M. Lammert, J.A. Dantzig, J. J.J. Coleman, J. Electron. Mater. 24 (1995) 1631.

44. J.F. Kluender, A.M. Jones, R.M. Lammert, J.E. Baker, J.J. Coleman, J. Electron. Mater. 25 (1996) 1514.

45. K. Kudo, T. Sasaki, M. Yamaguchi, J. Cryst. Growth 170 (1997) 634.

46. E.J. Thrush, J.P. Stagg, M.A. Gibbbon, R.E. Mallard, B. Hamilton, J.M. Jowett, E.M. Allen, Mater. Sci. Eng. B21 (1993) 130.

47. S. Ando, T. Hondo, N. Kobayashi, Appl. Phys. Lett. 32 (1993) L104.

48. J.E. Greenspan, X. Zhang, N. Puetz, B. Emmerstorfer, J. Vac. Sci. Tech. A 18 (2000) 648.

49. T. Sasaki, M. Kitamura, I. Mito, J. Cryst. Growth 132 (1993) 435.

50. M. Gibbon, J.P. Stagg, C.G. Cureton, E.J. Thrush, C.J. Jones, R.E. Mallard, R.E. Pritchard, N. Collis, A. Chew, Semiconduct. Sci. Tech. 8 (1993) 998.

51. Y. Kato, S. Kitamura, N.S. K. Hiramatsu, J. Cryst. Growth 144 (1994) 133.

52. R.J. Shul, C.G. Willison, L. Zhang, SPIE 3511 (1998) 252.

53. X. Li, A.M. Jones, S.D. Roh, D.A. Turnbull, E.E. Reuter, S.Q. Gu, S.G. Bishop, J.J. Coleman, Mat. Res. Soc. Symp. Proc. 395 (1996) 943.

54. J. Wang, R.S.Q. Fareed, M. Hao, S. Mahanty, S. Tottori, Y. Ishikawa, T. Sugahara, Y. Morishima, K. Nishino, M. Osinski, S. Sakai, Journal of Applied Physics 85 (1999) 1895.

55. T. Takeuchi, H. Amano, K. Hiramatsu, N. Sawaki, I. Akasaki, J. Cryst. Growth 115 (1991) 634.

56. A. Watanabe, T. Takeuchi, K. Hirosawa, H. Amano, K. Hiramatsu, I. Akasaki, J. Cryst. Growth 128 (1993) 391.